
UCRL-JRNL-423847

# Laser supported solid state absorption fronts in silica

*C. W. Carr and J. D. Bude*

**February 17, 2010**

Physical Review B

# Laser supported solid state absorption fronts in silica

C.W. Carr and J.D. Bude
*Lawrence Livermore National Laboratory, 7000 East Ave., Livermore, CA 94550*
(Received

We develop a model based on simulation and experiment that explains the behavior of solid-state laser-supported absorption fronts generated in fused silica during high intensity (up to 5GW/cm$^2$) laser exposure. We find that the absorption front velocity is constant in time and is nearly linear in laser intensity. Further, this model can explain the dependence of laser damage site size on these parameters. This behavior is driven principally by the temperature-activated deep sub band-gap optical absorptivity, free electron transport and thermal diffusion in defect-free silica for temperatures up to 15,000K and pressures < 15GPa. The regime of parameter space critical to this problem spans and extends that measured by other means. It serves as a platform for understanding general laser-matter interactions in dielectrics under a variety of conditions.

Understanding laser-induced damage has important practical applications in fields from telecommunications to inertial confinement fusion[1-4]. Although much work has been done to characterize the behavior of optical damage as a function of parameters such as laser pulse shape, and photon energy ($E_v$), the size and growth of damage sites generated during laser exposure is governed by the physics of laser-matter interactions under extreme conditions where material response is not well understood.

Recently, it was shown that for relatively low intensities (<10GW/cm$^2$) the size of laser initiated surface sites on fused silica (silica) optics scales approximately linearly with pulse duration[5]. In this work we explain this unexpected result with a computational model experimentally verified with shaped-pulse damage experiments. We show through modeling and experiment that a laser-supported absorption front (AF) is generated in the bulk silica during damage, and that it propagates linearly in time away from the absorbing precursor. For laser intensities, $I_L$, up to about 4GW/cm$^2$, the velocity of the front is nearly linear in $I_L$. This behavior is driven principally by the temperature-activated deep sub band-gap (3.55eV) absorptivity ($\alpha$), free electron (FE) transport and thermal diffusion of silica for temperatures (T) up to 15,000K and pressures (P) < 15GPa. The regime of parameter space critical to this problem spans and extends that measured by other means: direct measurements of T-activated $\alpha$ for photon energies > 6.5eV and T < 1,900K[6], and thermal diffusivity inferred from shock experiments for T>5,000K and P>70GPa[7].

Laser damage is a complex event comprising numerous phases from initiation to material ejection and fracture[8, 9]. This work focuses on energy deposition after initiation which is related to formation of a molten core[10]. Many models for laser damage have hypothesized that the dielectric is damaged when an extrinsic precursor absorbs enough sub $E_G$ light to reach a T high enough to induce further absorption in the host material resulting in mechanical damage[11-13]. The size of these precursors on high quality silica surfaces can be estimated from[5]. These measurements showed that damage site diameter, D, scales with pulse length, $\tau$, for fluences, $\phi=\tau I_L$ up to 20J/cm$^2$ and for $\tau$ as low as 200ps. For 200ps pulses, D~250nm, so these precursors must be < 250nm in size. T during a damage event has been measured as high as 12,000K [14]. We therefore model the state of a damage site immediately after initiation as a 200nm thick heated region located at the surface.

T-activated absorptivity has been found to play an important role in laser damage[15]. Measurements in[15] show that surface damage in silica can be generated without extrinsic absorbers far below the bulk material damage threshold when the surface is heated to T~2,200K using $\phi$=20J/cm$^2$, $\tau$=7ns, $E_v$=3.55eV pulses. This indicates that the absorptivity of defect-free intrinsic silica, $\alpha_{INT}(T)$, increases strongly with T. Under those conditions, $I_L\alpha_{INT}(2{,}200K)$ is sufficient to generate thermal run-away: when the defect absorption raises the precursor T high enough, the bulk silica becomes absorbing; absorption by the silica increases T which increases $\alpha_{INT}(T)$ leading to destructively high T. Laser damage of absorbing nanoparticles embedded in silica also suggests that silica becomes absorbing at high T[16]. Once the silica becomes absorbing, longer more energetic pulses feed increased energy deposition and would be expected to generate larger sites.

In this work, we use the following computational model (1) to understand energy deposition after initiation in a system with T-activated absorption. In (1) we simulate energy deposition, heat flow and photon transport in 1D. Although this model does not include material motion (hydrodynamic effects) and is only 1D, we show that it captures the salient behavior measured. We solve the following:

$$(C_V(T)\rho)\frac{\partial T}{\partial t} = \nabla \bullet (\kappa_{PH}(T)\nabla T) + G_{FE}(x) + I_L\alpha_{INT}(T) \qquad (1)$$

$$\frac{\partial I}{\partial x} = -\, I_L\alpha_{INT}(T)$$

where $\kappa_{PH}(T)$ is the silica phonon thermal conductivity, $C_V(T)$ is the silica heat capacity, and $\rho$ is density (values for T up to ~2,000K from[17]); t is time during the laser pulse, and x is

position below the surface. As previsouly noted, we assume initiation has just occurred at t=0, so we employ the initial boundary condition T(x,t=0)=9,000K for x<200nm. $C_V(T)$ is modeled as in[7] for T>10,000K. $G_{FE}$ is defined below. Radiative and evaporative cooling is included at the surface, but under the conditions studies had little effect on energy deposition during the pulse. $I_L$ is the laser intensity (constant in t) which propagates through the bulk towards the surface.

We adopt a model for $\alpha_{INT}(T)$ based on vibrational band edge distortion. As the T of a dielectric increases, phonon vibrations generate transient structural disorder forming localized electronic states in the gap (an exponentially decaying Urbach tail). The tail states are separated from continuum free-electron (FE) states by the "optical gap" $E_O$ which shrinks with increasing T ($E_G$ narrowing). For absorption of a phonon of energy $E_v$, this behavior is often modeled as:

$$\alpha_{INT}(E_v) \propto \exp(E_\upsilon / E_u) \qquad E_\upsilon < E_o \qquad (2)$$
$$\propto (E_\upsilon - E_o)^2 / E_\upsilon \qquad E_\upsilon \geq E_O$$

where $E_O(T)=E_G-AT$, $E_U(T) = B + CT$, $E_G$~9eV is the low T band gap, and A,B and C are constants. This behavior has been verified for $E_v$ < 6.5eV and T<1,900K. We assume it can be extended to higher T and lower $E_v$=3.55eV, and that $E_O$ and $E_U$ continue to behave linearly with respect to T with A=1e-3eV/K and B=0.02eV from[6]; we normalize $\alpha_{INT}$ to be consistent with[6] under the conditions measured there. For the conditions of[15] where the silica surface is heated to 2,200K, damage occurs only due to intrinsic absorption; we fit C so that $\alpha_{INT}$(2,200K) is large enough to support thermal runaway under these conditions. We find C=1.8x10$^{-4}$eV/K, close to C=1.4x10$^{-4}$ from[6]. Fig 1a shows the resulting $\alpha_{INT}(T)$ with $E_v$=3.55eV.

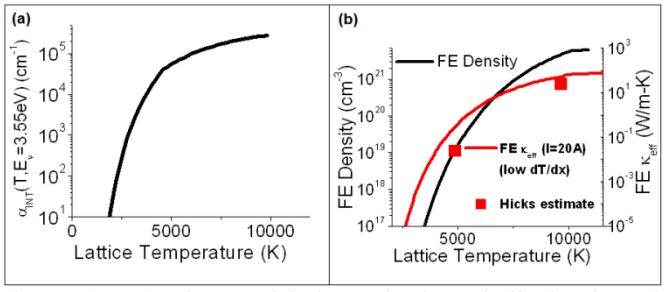


Fig. 1: (a) $\alpha_{INT}(T)$ from model; (b) FE density and effective thermal conductivity $\kappa_{eff}$ compared to [Hicks].

As $E_O$ shrinks with T, FE states are thermally populated. To be consistent with $\alpha_{INT}(T)$, the conduction and valence bands, $E_C$ and $E_V$, follow the optical gap: $E_C$-$E_V$=$E_O$. We assume the Fermi level, $E_F$=0, is in the middle of the optical gap, so that $E_C(T)$-$E_F$=$E_0(T)$/2. The FE density of states, the wave-vector (k) dependent velocity, v(k), and FE energy relative to the band edge, E(k), are computed using a simple effective mass approximation fit to the silica band structure [18]. This model predicts that FE densities increase dramatically between 5,000K and 10,000K (Fig. 1b), in accord with optical reflectivity measurements from shocks in silica which indicate an exponential increase in FE density at high P (70-1,000GPa) for T in that range[7]. Note: FE adds to $\alpha_{INT}$, but we assume that the direct band edge contribution dominates, especially as the gap narrows.

It should be Noted that FEs do not freely diffuse from hot regions to cold regions due to a large increase in $E_C(T)$ from high to low T – the band edge presents a thermionic emission energy barrier with a strong opposing electrical field[19]. However, these FEs do add to the thermal transport from phonon diffusion. Fig 2 shows the band edges at grid points x-$l$, and x, where $l$ is the mean free path for thermal electrons to give up their energy to the lattice. (All quantities including T and $E_C(T)$ are assumed piecewise constant at a grid point). These barriers are high since solution of (1) produces thermal gradients, $\partial T/\partial x$, as large as $10^6$K/um. Proper treatment requires the Boltzmann transport equation. To treat large $\partial T/\partial x$ with a differential equation formalism, we approximate the energy current, $J_{FE}(x_1:x_2)$, from $x_1$=x-$l$ to $x_2$=x using equation (3) where $v_x(k)$ is velocity in the x-direction, and $\Theta$ is the Heaviside function. Then, with a grid spacing =$l$, the net energy transport into a point x due to FEs diffusing from x-$l$ and x+$l$ (one energy loss mean-free path) can be approximated as $G_{FE}(x)$ in (3). We estimate $l$ =1nm to 5nm [18]. We define a FE $\kappa_{eff}$ (Fig 1b) for small $\partial T/\partial x$ in the limit where $G_{FE}(x) \rightarrow \kappa_{eff}(T)\ \partial^2 T/\partial x^2$. $\kappa_{eff}(T)$ is clearly T-activated and compares well with that inferred from[7]. As shown below, simulations under the conditions here are only weakly dependent on $l$.

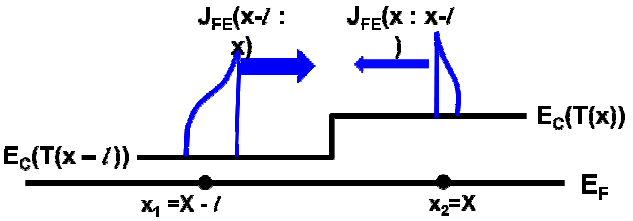


Fig 2: Flow of heat due to FE diffusion across the energy barrier between grid points x-$l$ and x with $E_F$=0. FE energy distributions and energy current shown in blue; energy shown vertically.

$$J_{FE}(x_1:x_2) = \int_0^\infty d^3k \frac{v_x(k)\ [E(k)-E_C(x_2)]\,\Theta[E(k)-E_C(x_2)]\Theta[v_x(k)]}{\exp[(E(k)+E_C(x_1))/k_BT(x_1)]+1}$$
$$G_{FE}(x) = [J(x-l:x)-J(x:x-l)+J(x+l:x)-J(x:x+l)]/l \qquad (3)$$

Simulations were performed for two cases: with only phonon diffusion ($G_{FE}$=0) and with both phonon and FE thermal diffusion. Fig. 3a shows results for $I_L$=1GW/cm$^2$. The 9,000K surface layer (precursor) activates $\alpha_{INT}$(T,x=0) leading to high energy deposition. As the surface layer get hotter, heat diffusion begins to activate $\alpha_{INT}$(T,x=δ) at points just next to the layer. T(x=δ) increases beyond 10,000K, and pushes energy deposition back further. This process continues while the laser is on, and the combination of T-activated absorption and heat diffusion creates a laser-supported solid-state AF. These AFs are qualitatively similar to laser supported combustion waves propagating in gasses[20], and the solid state propagating fiber-fuse effect in silica fibers[21].

As shown in Fig. 3b, the position of this front, $X_{4000}$, defined as the depth where T > 4,000K (>>boiling point) for

$x \leq X_{4000}$, moves linearly with time resulting in a constant AF velocity of $V_F = dX_{4000}/dt$. Because nearly all of the laser energy is absorbed by the AF, the maximum AF temperature ($T_{max}$) and $V_F$ are related: $I_L \propto T_{max} V_F$. Although phonon diffusion alone drives a front, it moves much more slowly than when FE diffusion is included. In fact, $V_F \propto I_L^{0.5}$ with only phonons, whereas with FE diffusion, $V_F \propto I_L^{0.8}$. When the FE component becomes large (T >10,000K), energy rapidly diffuses into the adjacent cool region, pinning $T_{max}$ near 10,000K – close to the black-body measurements of[14]. Because $T_{max}$ can then only increase weakly with $I_L$, and $I_L \propto T_{max} V_F$, $V_F$ becomes nearly linear in $I_L$. Phonon-only diffusion allows both $T_{max}$ and $V_F$ to increase together, and $T_{max}$ can then become much larger (>40,000K) than[14]. For laser intensities simulated here, radiative and evaporative cooling were found to have little effect on energy deposition during the pulse.

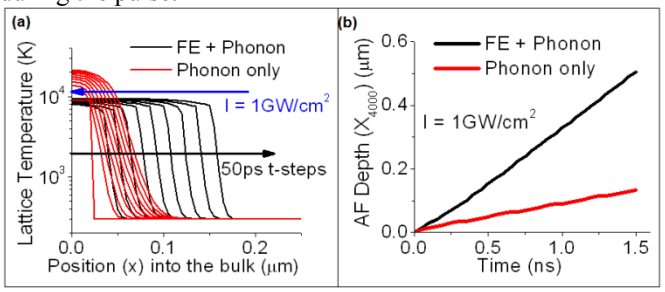


Figure 3: (a) time evolution of the AF (T(x) shown in 50ps intervals) with phonon diffusion only and with FE and phonon thermal diffusion; (b) formation of a constant front velocity, $V_F$.

In order to compare these 1D simulated results to measured laser damage sites, we assume that AF expansion occurs roughly spherically about the precursor; this would form a hemisphere of superheated (T>>boiling point) material on the surface. As long as there is a photon density to feed it, AF growth follows thermal diffusion ($\nabla T$), which should evolve linearly in time in all directions away from the heated precursor. This is supported by preliminary 3D hydrodynamics simulations which include a $\alpha_{INT}(T)$ term[22], and as shown below, by agreement seen with measurement. Eventually the superheated material will leave the surface through explosive boiling or fast evaporation. At the end of the pulse ($I_L \rightarrow 0$), the laser no longer drives the AF, and little further thermal diffusion occurs; therefore, laser damage should leave a molten "core" roughly the size of the superheated zone (extent of the AF). Consequently, the core radius should be related to the AF depth, and the core of the resulting laser damage site should grow linearly with time. Here, we compare simulated $V_F$ with the trends in rate of increase in the core radius with time.

Linear AF growth is consistent with measurements of damage site diameter, D, versus pulse length, τ[5]. However, the interpretation in[5] is complicated by the initiation condition – for a given τ, it is unclear how much of the laser pulse time is required to initiate the precursor (activate $\alpha_{INT}$), and how much grows the site to its final size (final superheated region). Also, D reported in [5] included the entire fracture zone surrounding the molten core[10]. The shaped pulse experiments described below with SEM images of the molten cores eliminate these issues.

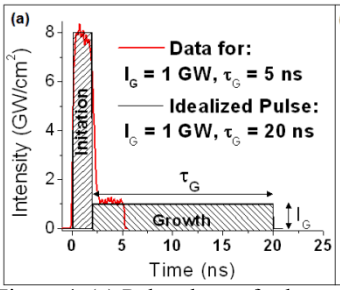


(b)

| Figure | $I_G$ (GW/cm²) | $\tau_G$ (ns) | $V_F$ (μm/ns) |
|---|---|---|---|
| A | 0 | - | - |
| B | 0.25 | 5 | 0.07 |
| C | 0.25 | 20 | - |
| D | 0.5 | 5 | 0.19 |
| E | 1.0 | 5 | 0.37 |
| F | 2.0 | 5 | 0.73 |

Figure 4: (a) Pulse shapes for laser damage: 2ns $I_0$=8GW/cm² control initiation pulse, with various growth "feet" defined by their intensity $I_G$ and duration $\tau_G$. (b) table of growth feet used to generate the sites in figure 5 a-f with the resultant velocity of the growth front.

First, 2" diameter, polished fused silica windows (CVI-Melles Groit) were cleaned with detergent and an ultra-sonic DI water rinse. Then damage was created with a (control) flat-in-time 3.55eV laser pulse with τ=2ns, $I_0$=8GW/cm² (Fig.4a).[23] As in the simulation, the laser pulse passed through the bulk, and damage on the exit surface was characterized. These conditions initiated about ~100 damage sites/cm² with an average site including surrounding fracture (fig. 5) of about 8um. Then, SEM images were taken of isolated surface sites (fig 5A). An easily identifiable molten core (herein, D is the core diameter) with ejecta fibers was found in most sites. The average D of 16 of these sites was 2.1um +/- 0.35um, and is indicated by the solid blue circle in fig. 5A. Thus, the 2ns initiation pulse reproducibly generates initiations with a small (D~2um) superheated surface zone; this is modeled as the initial 9,000K surface condition in the simulations.

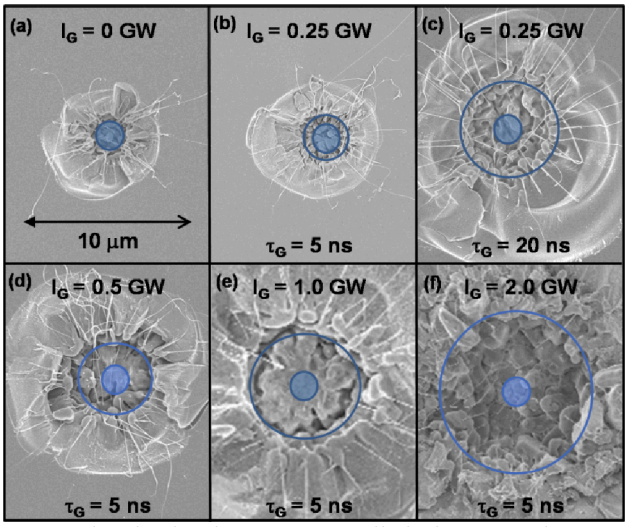


Figure 5: The size bar is common to all six images. The core is identified as the molten region in the SEM images which show the evidence of explosive ejection. Images a-f refer to the pulse shapes in Fig 4: (a-c) fixed $I_G$, increasing $\tau_G$; (d-f) fixed $\tau_G$, increasing $I_G$. In each image, the solid blue circle indicates the average measured control D. The outer blue circle indicates the average measured D of the core under different growth pulse conditions.

Then, a series of pulse shapes were explored in which the 2ns initiation pulse was followed by constant intensity AF growth "feet" which drive the expansion of the superheated zone. Various growth intensities, $I_G$ (≤6GW/cm$^2$), and duration $\tau_G$ (≤20ns) were explored to compare with the simulations above. $I_G$ plays the role of $I_L$ in the simulations.

The D of 10 or more sites for each condition was determined by SEM. The core diameters (Fig. 6a and Fig 5A-C) show a linear dependence on $\tau_G$ for constant $I_G$ corresponding to the model results (Fig. 3b). $V_F$ for these experiments is defined in analogy with the model; the experimental $V_F$ is the rate of increase in radius of the core due to the foot: $V_F=(R_G-R_C)/\tau_G$, where $R_G$ is the radius of the core generated with the growth pulse, and $R_C$ is the radius of the control core.

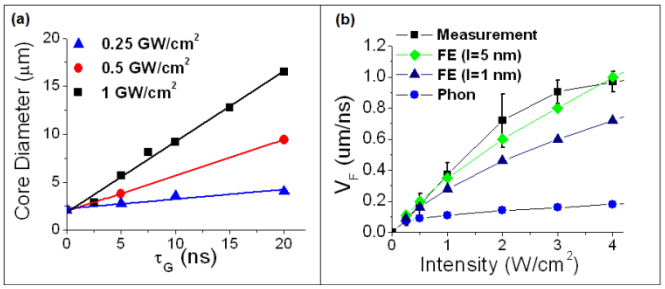


Figure 6: (a) experimental core diameters, D, versus intensity and $\tau_G$. (b) comparison of modeled and experimental $V_F$, with FE indicating the full free-electron + Phonon model with absorption depths of 1 and 5 nm, respectively. Phon is the phonon only model.

Fig. 6b directly compares the measured $V_F$ with modeled $V_F$ for driving $I_F$ up to 4GW/cm$^2$. Measured $V_F$ is shown along with error-bars. Note, under these conditions, $V_F$ is substantially lower than the speed of sound in silica (5.8um/ns), so the AF doesn't follow a shock. Instead, $V_F$ is much closer to the modeled results. Here, simulations were performed with phonon-only, and FE + phonon thermal diffusion. For the FE+phonon simulations, values of 1nm and 5nm were used for the energy-loss mean free path, *l*. While measurements and both models give constant $V_F$, the phonon-only thermal diffusion model under-predicts measurement by more than a factor of three at 1GW/cm$^2$ and has the wrong behavior versus $I_L$; measurements are much closer to the $V_F \propto I_L^{0.8}$ behavior when FE thermal diffusion is added, and the numerical agreement gets much closer. Note, that the propagation of the AF is not very sensitive to *l*; a factor of 5 change in *l* makes only ~35% change in $V_F$. In fact, modeled $V_F$ is a weak function of quantities like *l* which are most uncertain. Scaling $G_{TE}$ by a factor of ten around that used here only changes $V_F$ by ~30%. $V_F$ is most sensitive to the value $\alpha_{INT}$ attains at the maximum simulated temperature, $T_{max}$:$V_F \propto (\alpha_{INT}(T_{max}))^{0.5}$. $T_{max}$ with the phonon-only model can exceed 50,000K, but is in much better agreement with[14] using the FE model: 8,000K ($I_G$=0.25GW/cm$^2$) to 13,000K ($I_G$=5GW/cm$^2$). For T<15,000K, pressures are expected to be significantly < 15Pa[22, 24] , which suggests that hydrodynamic motion during energy deposition shouldn't influence AF behavior.

At higher $I_G$ (>5GW/cm$^2$), the measurements begin to show a saturation in $V_F$, whereas the model $V_F$ continues to increase. The cores become less distinct, and in many cases, the site morphology is dominated by deep and extensive fracture. This behavior may be explained by a complex material response to deep superheated material, and accurate modeling probably requires a 3D treatment including hydrodynamics and fracture.

Here we present a model for constant velocity solid-state laser-supported AFs in FS. This model is supported by laser damage experiments and numerical simulation. In general, solid-state absorption fronts will result from the combination of high T activated $\alpha_{INT}(T)$ and thermal conductivity. This is expected to happen in any material with these properties. Good agreement between simulation and experiment was found by extending models $\alpha_{INT}(T)$ based on Urbach broadening and band-gap narrowing which include high thermal conductivity from FE generation. This model is consistent with a variety of other experiments including direct silica absorptivity measurements performed up to 1900K, shock measurements of optical reflectivity in silica, and high T damage experiments on silica surfaces. This model extends our understanding of the absorptivity and thermal diffusivity of silica for a range of T and P not well understood. This model serves as a platform for understanding general laser-matter interactions in dielectrics including laser-supported solid-state AFs in a variety of materials and under various conditions[20, 21].

The authors would like to thank M.L Spaeth, B. Sadigh, P. Demange, J. Stolken, M.D. Feit and the crew of OSL for their assistance in this work This work is performed under the auspices of the U.S. Department of Energy by Lawrence Livermore National Laboratory under Contract DE-AC52-07NA27344 and funded through LLNL office of LDRD. (LLNL-NNN-xxxxxx).

[1] C. W. Carr, *et al.*, Meas. Sci. & Tech. **17**, 1958 (2006).
[2] M. Ushio, *et al.*, Shock Waves **18**, 35 (2008).
[3] S. I. Yakovlenko, Laser Physics **16**, 1273 (2006).
[4] J. D. Lindl, *et al.*, Physics of Plasmas **11**, 339 (2004).
[5] C. W. Carr, *et al.*,SPIE **6403**, K4030 (2007).
[6] K. Saito, *et al.*, Physical Review B **62**, 8584 (2000).
[7] D. G. Hicks, *et al.*, Physical Review Letters **97** (2006).
[8] C. W. Carr, *et al.*, Optics Letters **31**, 595 (2006).
[9] R. A. Negres, *et al.*,SPIE **6720**, 72019 (2008).
[10] C. W. Carr, *et al.*, Applied Physics Letters **89** (2006).
[11] C. W. Carr, *et al.*, Physical Review Letters **91** (2003).
[12] M. D. Feit, *et al.*,SPIE **5273**, 74 (2004).
[13] S. Palmier, *et al.*, SPIE **6720**, U576 (2008).
[14] C. W. Carr, *et al.*, Phys. Rev. Letters **92**, 087401 (2004).
[15] J. D. Bude,SPIE **6403**, 67209 (2007).
[16] S. Papernov, *et al.*, J. Applied Physics **92**, 5720 (2002).
[17] S. T. Yang, *et al.*, J. App. Physics **106**, 103106 (2009).
[18] D. Arnold, *et al.*, Physical Review B **46**, 15102 (1992).
[19] K. Hess, *Theory of Semiconductor Devices* (IEEE Press Marketing, Piscataway, NJ, 2000).
[20] M. v. Allmen, *Laser-Beam Interactions with Materials* (Springer, Lexington, MA, 1987).
[21] D. P. Hand, *et al.*, Optics Letters **13**, 767 (1988).
[22] P. De Mange, 2009), p. Hydrodynamics simulations.
[23] M. C. Nostrand, *et al.*,SPIE **5273**, 325 (2003).
[24] D. E. Hare, *et al.*, 2009), p. CALE EOS from 2 fits for high pressure fuesed silica Hugoniot data.